Effect of electron-hole separation on the Landau-level photoluminescence in layered structures in a tilted magnetic field: Magneto-Stark effect

S. K. Lyo
Sandia National Laboratories, Albuquerque, New Mexico 87185
(Received 11 May 1998; revised manuscript received 24 July 1998)

We show that the photoluminescence (PL) intensities of the interband transitions between the electron and hole Landau levels ($n_e, n_h = 0,1,...$) in a perpendicular magnetic field $B_\perp$ are modulated strongly by a superimposed in-plane field $B_\parallel$ in type-II quantum wells due to electron-hole separation: $B_\parallel$ suppresses the intensities of the $n_e \to n_h = n_e$ diagonal transitions initially and generates $n_e \to n_h \neq n_e$ off-diagonal transitions that are forbidden at $B_\parallel = 0$. The intensities oscillate at higher $B_\parallel$. An additional electric field $E_\parallel$ parallel to $B_\parallel$ modifies the effective $B_\parallel$ and introduces a magneto-Stark shift in the PL line. This new Stark shift requires $B_\parallel \neq 0$ unlike the ordinary Stark shift in perpendicular $E_\perp$. [S0163-1829(98)51040-5]

I. INTRODUCTION

Photoluminescence (PL) in quantizing magnetic fields has been a useful tool for investigating electronic structures of semiconductor quantum wells (QW's) and heterostructures.[1–3] In the presence of an applied magnetic field perpendicular to the QW plane, the electrons in *n*-doped systems and photogenerated holes are quantized into low-energy Landau levels (LL's) n_e and $n_h = 0,1,2...$. When the carrier temperature is high enough for the occupation of several valence-band LL's by the holes, the electron-hole recombination goes through the allowed $n_e \to n_h = n_e$ direct transitions. On the other hand, when all the holes are in the ground level $n_h = 0$ at low temperatures, the electron-hole recombination goes through the $n_e (= 0,1,2,...) \to n_h = 0$ transitions. In this case, the off-diagonal transitions ($n_e > 0$) are very weak because they are zeroth-order forbidden and occur only through higher-order processes involving impurity interactions.[4] Simultaneous determination of the electron and hole masses has been possible by combining the data from the direct and indirect transitions.[2] In this paper, we show that strong (i.e., zeroth-order allowed) off-diagonal transitions can be induced by applying an in-plane component $B_\parallel$ to the perpendicular field $B_\perp$, when the electrons are spatially separated from the holes. The theory is applied to a low-density sample at low temperatures where this effect can be observed.

Electron-hole separation occurs in many systems such as asymmetrically doped double quantum wells (DQW's), type-II heterostructures, or DQW's with a bias electric field $E_\perp$ applied in the growth (z) direction. In Fig. 1, we show a 57-46-53-Å GaAs/Al_xGa_{1-x}As DQW structure (sample 1), where the conduction and valence band edges are raised by 12 meV at the centers of the right QW's relative to those in the left QW's by $E_\perp = 11.9$ kV/cm. The electron-hole recombination is represented by a thick arrow. Recombination between the electrons and the holes trapped inside the left QW is also possible, yielding higher energy photons. These single-well transitions are well understood as discussed above and will not be discussed here. Unfortunately, there is no systematic technique available to determine the degree of the electron-hole separation. The $B_\parallel$-induced PL selection rules combined with the magneto-Stark shift predicted in the present theory can be utilized to determine the distance and the sign of the electron-hole separation.

In $\boldsymbol{B} = (B_\parallel, B_\perp)$, the intensities of the direct $n_e \to n_h = n_e$ transitions (allowed at $B_\parallel = 0$) decrease to zero initially and oscillate with increasing $B_\parallel$ under a fixed $B_\perp$. In contrast, the intensities of the off-diagonal $n_e \to n_h \neq n_e$ transitions (for-

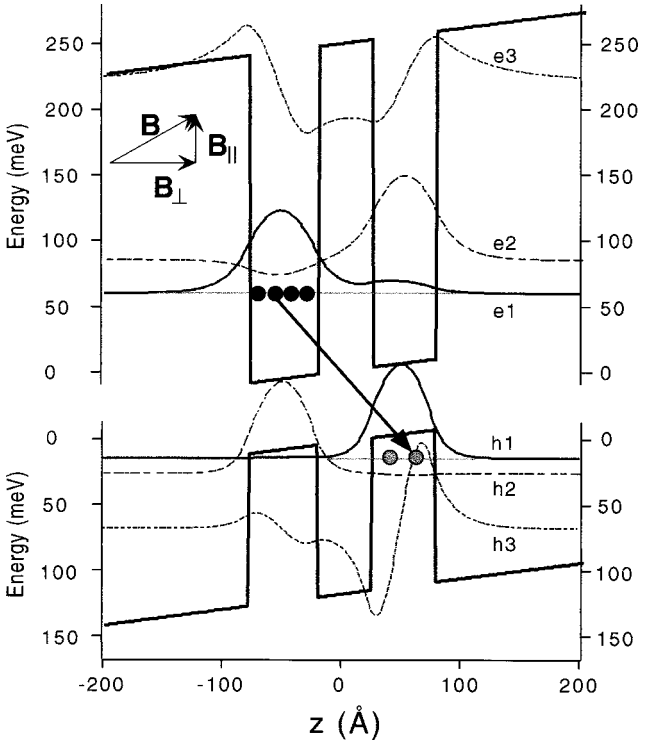

FIG. 1. A 57-46-53 Å GaAs/$Al_{0.3}Ga_{0.7}$As DQW structure (sample 1) with a $E_\perp = 11.9$ kV/cm bias in the z direction. The band offsets are 250 meV for the electrons and 116 meV for the heavy holes ($|3/2, \pm 3/2\rangle$). Light holes are not populated due to a larger confinement energy. The electrons (solid circles) and photogenerated holes (hatched circles) are separated by $d = 100$ Å. The wave functions are shifted by the amount of the sublevel energies. Other parameters are given in the text.

bidden at $B_\parallel=0$) increase from zero, reach maxima, and oscillate similarly with $B_\parallel$. The $B_\parallel$-dependent oscillations of the transition intensities are determined approximately by $B_\perp/d^2$ at low fields. Here d is the expectation value of the separation distance between the electrons and holes. The effect of an additional in-plane dc electric field $\boldsymbol{E}_\parallel$ applied in the x direction parallel to $\mathbf{B}_\parallel$ is to modify the effective $B_\parallel$ linearly and to introduce a magneto-Stark shift $deE_\parallel B_\parallel/B_\perp$ in the PL line. Here $e=|e|$ is the electronic charge. This unusual Stark shift requires a nonzero $B_\parallel$. It can be positive or negative and larger or smaller than the ordinary Stark shift induced by a purely perpendicular electric field $E_\perp=E_\parallel$.

II. SELECTION RULES AND MAGNETO-STARK SHIFT IN TILTED MAGNETIC FIELD

The Hamiltonian in a direct-gap structure is given by

$$H_\alpha=\frac{\hbar^2}{2m_\alpha^*}\left(k_y+\frac{e}{\hbar c}A_y\right)^2-\frac{\hbar^2}{2m_\alpha^*}\frac{\partial^2}{\partial x^2}+s_\alpha eE_\parallel x+H_{z,\alpha}, \tag{1}$$

where m_α^* is the effective mass, $s_e=1$ for the electrons, $s_h=-1$ for the holes, and $A_y=B_\perp x-B_\parallel z$ is the vector potential. The effect of the confinement Hamiltonian $H_{z,\alpha}$ in Eq. (1) is to confine the electron and hole ground-sublevel wave functions $|\alpha 1\rangle$ around $z_\alpha=\langle\alpha 1|z|\alpha 1\rangle$. Here the ith eigenstate of $H_{z,\alpha}$ is denoted as $|\alpha i\rangle$ (e.g., $e1$, $e2$, $h1$, $h2$,...). Only the ground sublevels $i=1$ are populated at low temperatures. We therefore approximate $z=z_\alpha$ in A_y. This approximation neglects (1) the LL-sublevel mixing in the limit the magnetic length $l_\parallel=(\hbar c/eB_\parallel)^{1/2}$ is larger than the QW width and (2) the field-induced distortion of $|\alpha 1\rangle$. This approximation is valid for small magnetic energies $\hbar\omega_{\perp\alpha}=eB_\perp/m_\alpha^* c$, $\hbar\omega_{\parallel\alpha}=eB_\parallel/m_\alpha^* c$. These conditions are satisfied in typical narrow QW's in magnetic fields up to several tesla. The accuracy of this approximation is assessed in Sec. III, where a full exact numerical solution is presented and the domain of validity is derived for the fields.

Equation (1) is then simplified to

$$H_\alpha^{(0)}=-\frac{\hbar^2}{2m_\alpha^*}\frac{\partial^2}{\partial x^2}+\tfrac{1}{2}m_\alpha^*\omega_{\perp\alpha}^2(x+x_\alpha)^2+\varepsilon_\alpha+H_{z,\alpha}, \tag{2}$$

where $x_\alpha=x_0+s_\alpha\delta x$,

$$\varepsilon_\alpha=-k_y s_\alpha eE_\parallel l_\perp^2+z_\alpha s_\alpha eE_\parallel B_\parallel/B_\perp-m_\alpha^*(eE_\parallel l_\perp^2/\hbar)^2/2, \tag{3}$$

$$x_0=k_y l_\perp^2-(z_e+z_h)B_\parallel/2B_\perp+(m_e^*-m_h^*)eE_\parallel l_\perp^4/2\hbar^2, \tag{4}$$

and

$$\delta x=z_{he}B_\parallel/2B_\perp+eE_\parallel l_\perp^2/2\hbar\omega_{\perp M}. \tag{5}$$

In Eqs. (2)–(5), $z_{he}=z_h-z_e$ is the algebraic distance between the electron and hole layers, $l_\perp=(\hbar c/eB_\perp)^{1/2}$, $\omega_{\perp M}=eB_\perp/Mc$, and $M=m_e^*+m_h^*$. The electron-hole separation is given by $d=|z_{he}|$. The eigenvalues of Eq. (2) are given by $\mathcal{E}_\alpha(n_\alpha,k_y)=\hbar\omega_{\perp\alpha}(n_\alpha+1/2)+\varepsilon_\alpha$. The resonance photon energy for the $n_e\to n_h$ transition is then given, apart from the gap plus the ground-sublevel energies of $H_{z,\alpha}$, by

$$\varepsilon_{\mathrm{PL}}(n_e\to n_h)=\hbar\omega_{\perp e}(n_e+\tfrac{1}{2})+\hbar\omega_{\perp h}(n_h+\tfrac{1}{2})+\Delta\varepsilon, \tag{6}$$

where

$$\Delta\varepsilon=-z_{he}eE_\parallel B_\parallel/B_\perp-(eE_\parallel l_\perp)^2/2\hbar\omega_{\perp M}. \tag{7}$$

Note that the sign of the magneto-Stark shift, namely, the first term of $\Delta\varepsilon$ in Eq. (7), depends on the signs of z_{he} and $E_\parallel$. This unusual Stark shift requires a nonzero $B_\parallel$ and can be larger or smaller than the ordinary Stark shift induced by $E_\perp$ depending on the relative magnitudes of $B_\parallel$ and $B_\perp$. The quadratic term in Eq. (7) was obtained earlier by Aronov[5] for bulk semiconductors in the crossed fields of **E** and **B** and is much smaller than the linear magneto-Stark shift term for small $E_\parallel$.

The origin of the magneto-Stark shift is understood in the following way. The potential energies of an electron and a hole at the k_y-dependent part of the centroid $x=-x_{0,1}\equiv-k_y l_\perp^2$ are given by $-x_{0,1}s_\alpha eE_\parallel=-s_\alpha k_y l_\perp^2 eE_\parallel$, which is the first term on the right-hand side of Eq. (3). In the presence of $B_\parallel$, the wave number k_y is displaced by $\Delta k_y=-z_\alpha/l_\parallel^2$, yielding a shift $s_\alpha z_\alpha l_\perp^2 eE_\parallel/l_\parallel^2=s_\alpha z_\alpha eE_\parallel B_\parallel/B_\perp$. The latter is the shift of the potential energy of the electrons and holes at the centroid of the wave function due to $B_\parallel$ and $E_\parallel$. This is the second term on the right-hand side of Eq. (3). The magneto-Stark shift for the PL energy is the sum of the contributions from the electron and the hole.

The eigenfunctions of Eq. (2) are the harmonic functions $\varphi_n(x+x_\alpha)$ with the centroid at $x=-x_\alpha$. The total wave function is given by $\Psi_\alpha=L_y^{-1/2}\exp(-ik_y y)\varphi_{n_\alpha}(x+x_\alpha)|\alpha 1\rangle$, where L_y is the length of the sample in the y direction. The argument $x_\alpha=x_0+s_\alpha\delta x$ contains a uniform part x_0 and a relative part $s_\alpha\delta x$. The role of δx is then to shift the harmonic wave functions of the electrons and holes relative to each other, introducing oscillations in the overlap function $\langle\phi_{n_e}(x+\delta x)|\phi_{n_h}(x-\delta x)\rangle$. The probability $P(\xi)$ for the $n_e\to n_h$ transition is proportional to $|\langle\Psi_e|\Psi_h\rangle|^2$ and equals, apart from the overlap factor $\langle h1,e1\rangle^2$,[6]

$$P_{n_e,n_h}(\xi)=P_{n_h,n_e}(\xi)=|\langle\varphi_{n_e}(x+\delta x)|\varphi_{n_h}(x-\delta x)\rangle|^2$$

$$=\frac{n_<!}{n_>!}e^{-\xi}\xi^{(n_>-n_<)}L_{n_<}^{n_>-n_<}(\xi)^2, \tag{8}$$

where $\xi=2(\delta x/l_\perp)^2$ is dimensionless, $n_>(n_<)$ is the larger (lesser) of (n_e,n_h), and $L_n^m(\xi)$ is the associated Laguerre polynomial. The first term of δx in Eq. (5) is proportional to d. The effect of the second term linear in $E_\parallel$ has been studied earlier by Aronov[5] in bulk semi-conductors in the crossed fields of **E** and **B** and is independent of d.

In Fig. 2, we plot the relative transition probability $P_{n,n'}(\xi)$ for sample 1 (i.e., $d=100$ Å) in dashed curves as a function of $B_\parallel$ for low-lying levels $n=n_e$ and $n'=n_h$ and $E_\parallel=0$. At $B_\parallel=\xi=0$, the probability $P_{n,n'}(\xi)$ equals unity for the $n\to n$ direct transitions and vanishes for the off-diagonal transitions $n_e\to n_h\neq n_e$. The $B_\parallel$-dependent oscillations arise from (1) the orthonormality of the harmonic wave functions in the conduction and valence bands and (2) the relative $B_\parallel$-induced displacement δx of the centroid of the harmonic wave functions of the electrons and holes due to their separation. The effect of $E_\parallel$ is to linearly shift the effective $B_\parallel$ for the oscillations according to Eq. (5).

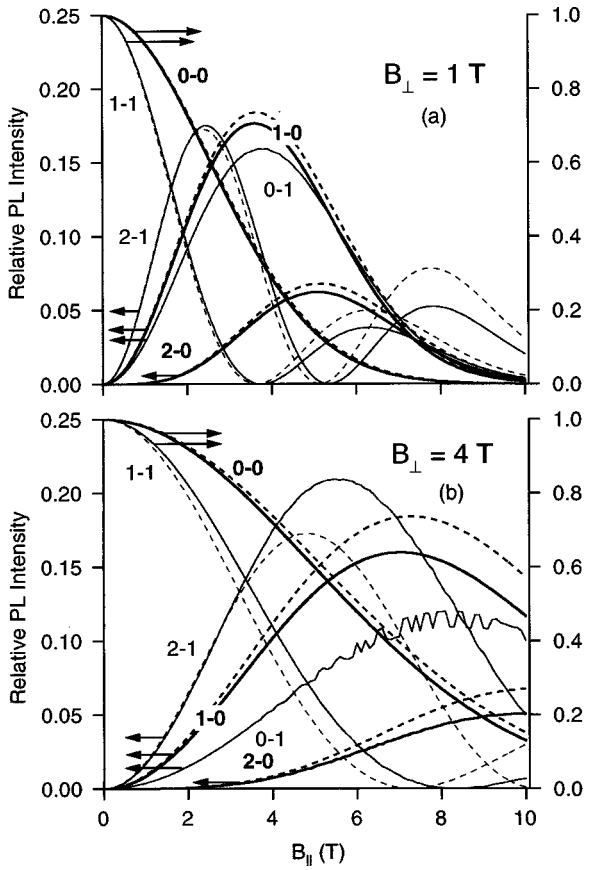

FIG. 2. Relative PL intensity for direct $n_e \rightarrow n_h$ transitions for (a) $B_\perp = 1$ T and (b) $B_\perp = 4$ T for sample 1 with $d = 100$ Å and $E_\parallel = 0$. The dashed curves are from $P_{n,n'}(\xi)$ and the solid curves are from the full numerical solution. Zero-temperature transitions for an n-type sample are marked by bold labels and thick solid lines. The wriggles for the 0-1 curve in (b) are from numerical fluctuations.

III. DOMAIN OF VALIDITY AND FULL NUMERICAL SOLUTION

In this section, we give an exact numerical solution for the total Hamiltonian, assess the accuracy of the analytic results in Sec. II, and derive the domain of their validity. These results were obtained by approximating $z = z_\alpha$ in Eq. (1). The correction term is given by

$$H_\alpha^{(1)} = m_\alpha^* \omega_{\parallel\alpha}^2 (z - z_\alpha)^2/2 + s_\alpha m_\alpha^* \omega_{\parallel\alpha} e E_\parallel l_\perp^2 (z - z_\alpha)/\hbar - m_\alpha^* \omega_{\perp\alpha} \omega_{\parallel\alpha} (x + x_\alpha)(z - z_\alpha). \quad (9)$$

The total Hamiltonian $H_\alpha = H_\alpha^{(0)} + H_\alpha^{(1)}$ can be diagonalized using $\varphi_{n_\alpha}(x + x_\alpha)|\alpha i\rangle$ as a basis set. It is sufficient to use several LL's and two to three sublevels. The first two terms in Eq. (9) are diagonal in $\varphi_{n_\alpha}(x + x_\alpha)$ and the last term has off-diagonal matrix elements $\langle n|x + x_\alpha|n'\rangle = l_\perp(\sqrt{n}\,\delta_{n',n-1} + \sqrt{n'}\,\delta_{n',n+1})/\sqrt{2}$. Before presenting full numerical solutions, we derive the conditions that the corrections caused by $H_\alpha^{(1)}$ are negligible.

The first-order correction from the first term in Eq. (9) should be much smaller than the LL energy:

$$\frac{(m_\alpha^*/4m_{z\alpha}^*)(\hbar\omega_{\parallel\alpha})^2}{\hbar^2/(2m_{z\alpha}^*\langle\alpha 1|(z - z_\alpha)^2|\alpha 1\rangle)} \ll \hbar\omega_{\perp\alpha}. \quad (10)$$

The denominator in Eq. (10) (defined as $Z_{\alpha\alpha}$) has an energy scale of the sublevel energies. For example, $Z_{\alpha\alpha} = 1.03\Delta\varepsilon_{z\alpha 2}$ for an infinitely deep QW and $Z_{\alpha\alpha} = \Delta\varepsilon_{z\alpha 2}$ for a parabolic QW, where $\Delta\varepsilon_{z\alpha i}$ is the separation between the ground and the ith sublevel. For sample 1, $Z_{ee} = 101.5$ meV and $Z_{hh} = 54.07$ meV, yielding $0.0043 \ll B_\perp/B_\parallel^2$ for the electrons and $0.0015 \ll B_\perp/B_\parallel^2$ for the holes. Here, **B** is in tesla. These conditions are easily satisfied except at extremely small $B_\perp$ and large $B_\parallel$. For the masses $m_e^* = m_{ze}^* = 0.067$ (in units of the free electron mass), $m_h^* = 0.11$, and $m_{zh}^* = 0.45$, the magnetic energies are $\hbar\omega_{\parallel e} = \hbar\omega_{\perp e} = 1.73$ meV, $\hbar\omega_{\parallel h} = \hbar\omega_{\perp h} = 1.06$ meV at $B_\parallel = B_\perp = 1$ T.

The second term in Eq. (9) yields a second-order correction $\equiv \lambda_1 \varepsilon_\alpha'''$ to ε_α''', which is the quadratic term (in $E_\parallel$) of ε_α in Eq. (3). This correction should be small:

$$\lambda_1 = \sum_{i>1} \frac{(m_\alpha^*/4m_{z\alpha}^*)(\hbar\omega_{\parallel\alpha})^2}{\Delta\varepsilon_{z\alpha}[\hbar^2/(2m_{z\alpha}^*\langle\alpha i|(z - z_\alpha)|\alpha 1\rangle^2)]} \ll 1. \quad (11)$$

Again, the energy in the square brackets in the denominator is large. For sample 1, Eq. (11) yields $B_\parallel \ll 36.1$ T and $B_\parallel \ll 92.2$ T, respectively, for the electrons and holes. These conditions are relevant only for the $E_\parallel^2$-dependent PL shift in Eq. (6).

For the n_αth LL, the third term in Eq. (9) yields a second-order correction $\equiv -\lambda_2 \hbar\omega_{\perp\alpha}$ which should be small:

$$\lambda_2 = \sum_{i>1,\pm} \times \frac{(m_\alpha^*/4m_{z\alpha}^*)(\hbar\omega_{\parallel\alpha})^2 n_{\alpha,\pm}}{(\Delta\varepsilon_{z\alpha i} \pm \hbar\omega_{\perp\alpha})[\hbar^2/(2m_{z\alpha}^*\langle\alpha i|(z - z_\alpha)|\alpha 1\rangle^2)]} \ll 1. \quad (12)$$

Here $n_{\alpha,\pm} = n_\alpha + 1/2 \pm 1/2$. For sample 1, Eq. (12) yields $B_\parallel \ll 69.5$ T and $B_\parallel \ll 144.6$ T for $n_\alpha = 0$ and $B_\perp = 4$ T for the electrons and holes, respectively.

We have also performed similar numerical studies for asymmetric 57-48-53-Å GaAs/$Al_{0.3}Ga_{0.7}$As DQW's with the same 12 meV mismatch between the left and right QW's as in sample 1 but with flat QW bottoms and with $E_\perp = 0$. Very similar numerical results were obtained.

In order to assess the accuracy of the approximate results in Sec. II, we have performed a full exact numerical diagonalization of the Hamiltonian H_α for sample 1, using four sublevels and ten LL's for both the electrons and holes. As expected from the error analysis presented in Eqs. (10)–(12), the fan (i.e., $\varepsilon_{PL}(n_e \rightarrow n_h)$ vs $B_\perp$) diagrams show no visible deviation from the slopes given by Eq. (6) below $B_\parallel$, $B_\perp < 10$ T for sample 1. Also, the shift of the PL energy at $B_\perp = 0$ is negligible below $B_\parallel = 5$ T, while it is about 0.6 and 0.3 meV for the electrons and holes at $B_\parallel = 10$ T. The full numerical transition probabilities (solid curves) are compared with $P_{n,n}(\xi)$ in Fig. 2 for $E_\parallel = 0$. Only the $n_e \rightarrow n_h = 0$ transitions (thick curves with bold labels) are relevant at low temperatures for an n-type sample. The deviation of the full numerical result from $P_{n,n}(\xi)$ is small at low fields as seen in Fig. 2(a). However, the deviation is significant at high

$B_\parallel$'s as seen above $B_\parallel = 4$ T in Fig. 2(b). In Fig. 2, the 0-1 transition shows more deviation than the 1-0 transition.

The corrections to $P_{n,n'}(\xi)$ at higher fields in Fig. 2 can be understood in the following way. The perturbation $H_\alpha^{(1)}$ admixes a small amount of higher-energy ($i>1$) sublevel states to $|\alpha 1\rangle$. The transition overlap integrals $|\langle h1|ei\rangle|$ and $|\langle hi|e1\rangle|$ of these higher-energy states are, however, much larger than $|\langle e1|h1\rangle|$, yielding a significant correction to $P_{n,n'}(\xi)$ outside the low field regime. The first two terms in Eq. (9) admix only the sublevels without affecting the LL state. The first-order effect of these terms is to modify the transition rate $n_e \rightarrow n_h$ by a factor $(1+\beta_1 B_\parallel^2 + \beta_2 E_\parallel B_\parallel / B_\perp)^2$, where $\beta_1 = -0.006$ and $\beta_2 = -0.057$ for sample 1 with $B_\parallel$, $B_\perp$ in units of T and in $E_\parallel$ units of 1 kV/cm. In contrast, the last term in Eq. (9) admixes the $n_e \pm 1$ st LL's to the initial n_eth LL, thereby adding ''$n_e \pm 1 \rightarrow n_h = 0$'' type oscillations to the $n_e \rightarrow n_h = 0$ PL transition. The PL energies are, however, given by Eq. (6) as long as the conditions in Eqs. (10)–(12) are satisfied.

IV. CONCLUSIONS

We have shown that the LL PL intensities in a tilted magnetic field $\mathbf{B} = (B_\parallel, B_\perp)$ depend strongly on $B_\parallel$ when the electrons and holes are separated. The intensities of the direct $n_e \rightarrow n_h = n_e$ transitions (allowed at $B_\parallel = 0$) decrease to zero initially and oscillate between zero value and maxima with increasing $B_\parallel$ under a fixed $B_\perp$. In contrast, the intensities of the off-diagonal $n_e \rightarrow n_h \neq n_e$ transitions (forbidden at $B_\parallel = 0$) increase from zero, reach a maximum, and oscillate similarly with $B_\parallel$. The in-plane dc electric field $E_\parallel$ modifies the overlap of the LL functions and introduces a linear magneto-Stark shift plus a quadratic shift given in Eq. (7) in the PL line. This unusual Stark shift requires a nonzero $B_\parallel$ and can be larger or smaller than the ordinary Stark shift. The results are applicable to thin type-II QW's where the electron and hole ground sublevels are spatially separated at low fields. The analytic results obtained in Sec. II are valid only for small $E_\parallel$, $B_\parallel$, and $B_\perp$ while the full exact numerical results in Sec. III show similar behavior outside this range as shown in Fig. 2. Rigorous criteria for the domains of validity of the fields for the PL energies given in Eq. (6) were presented in Eqs. (9)–(12).

An estimate of the relative separation of the electron and hole layers can be obtained from the magneto-PL data from the magneto-Stark shift as well as from the $B_\parallel$-dependent oscillations of the transition intensities at low fields. In type-II structures, however, the PL intensity is much weaker than in the type-I systems due to a small electron-hole overlap $\langle h1|e1\rangle$, unless either the electron or the hole effective mass is small enough to allow the confinement wave functions to penetrate deeply into the center barrier.

ACKNOWLEDGMENT

Sandia is a multiprogram laboratory operated by Sandia Corporation, a Lockheed Martin Company, for the U.S. DOE under Contract No. DE-AC04-94AL85000.

[1] J. M. Worlock, A. C. Maciel, A. Petrou, C. H. Perry, R. L. Aggarwal, M. Smith, and A. C. Gossard, Surf. Sci. **142**, 486 (1984).

[2] E. D. Jones, S. K. Lyo, I. J. Fritz, J. F. Klem, J. E. Schirber, C. P. Tiggs, and T. J. Drummond, Appl. Phys. Lett. **54**, 2227 (1989).

[3] M. S. Skolnick, K. J. Nash, S. J. Bass, P. E. Simmonds, and M. J. Kane, Solid State Commun. **67**, 637 (1988).

[4] S. K. Lyo, E. D. Jones, and J. F. Klem, Phys. Rev. Lett. **61**, 2265 (1988); S. K. Lyo, Phys. Rev. B **40**, 8418 (1989).

[5] A. G. Aronov, Fiz. Tverd. Tela (Leningrad) **5**, 552 (1963) [Sov. Phys. Solid State **5**, 402 (1963)].

[6] J. Hu and A. H. MacDonald, Phys. Rev. B **46**, 12 554 (1992).